the highest correlation coefficient. This method of fitting A_∞ to data spanning 1 half-life was compared, with the use of identical data sets, to the Guggenheim method (4 half-lives) and to a method in which A_∞ was calculated with the extinction coefficient of the product aryloxide for the reaction of KOEt with **1f**. Comparison of the two mean rate constants from the A_∞ (fitted) and Guggenheim methods showed that they were not statistically different at the 95% confidence level. However, the scatter in the results (95% confidence level) was about 4% of the mean for the fitted A_∞ method compared to 2% for the Guggenheim method. The fitting method was found to be more accurate than methods that use infinity absorbances calculated from extinction coefficients: The mean rate constant from the A_∞ (calculated) method differed by 12% from the mean rate constant from the Guggenheim method.

Anhydrous ethanol, 18-crown-6, lithium ethoxide, and potassium ethoxide were prepared and/or purified as described previously.[18]

Synthesis of Aryl Benzenesulfonates. Six esters were prepared following the general procedure of Davy et al.[35] Benzenesulfonyl chloride (2.6 mL, 0.02 mol) was dissolved in dry ether (100 mL), and redistilled Et_3N[36] (5 mL, 0.07 mol) was added. Next, the substituted phenol (0.022 mol) was dissolved in dry ether (100 mL) and added to the acid chloride solution. The reaction mixture was stirred under nitrogen; progress of the reaction was monitored by TLC, the reaction time generally being about 2 days. When the reaction was complete, the reaction mixture was worked up as follows: Et_3NHCl was filtered off and washed with dry ether, and then the ether solution was washed with 5% aqueous HCl solution (4 × 50 mL), 5% aqueous Na_2CO_3 solution (6 × 50 mL), and saturated aqueous NaCl solution (3 × 50 mL). The ether solution was dried over anhydrous Na_2SO_4, filtered, and concentrated under reduced pressure. The crude product was either repeatedly recrystallized from ethanol to a constant melting point (**1a-1c**, **1f**) or purified by fractional distillation under reduced pressure (**1d**; 146-155 °C at 0.35 mmHg).[37] Purified esters gave excellent ^1H and ^{13}C NMR spectra and IR spectra, as well as elemental analyses.

Acknowledgment. This research was supported by the Natural Sciences and Engineering Research Council of Canada (NSERC). The awards to M.J.P. of a Postgraduate Scholarship by NSERC and a Graduate Award by Queen's University are gratefully acknowledged.

Registry No. 1a, 3313-84-6; **1b**, 41076-06-6; **1c**, 132803-38-4; **1d**, 132803-39-5; **1e**, 80-38-6; **1f**, 4358-63-8; KOEt, 917-58-8; LiOEt, 2388-07-0; K^+, 24203-36-9; Li^+, 17341-24-1; $PhSO_2OCl$, 98-09-9; 18-crown-6, 17455-13-9.

Supplementary Material Available: Tables of kinetic data for the reactions of **1a-1f** with alkali-metal ethoxides, as well as observed and literature values of melting points of the esters (5 pages). Ordering information is given on any current masthead page.

(35) Davy, M. B.; Douglas, K. T.; Loran, J. S. A.; Steltner, A.; Williams, A. *J. Am. Chem. Soc.* **1977**, *99*, 1196.
(36) Crossland, R. K.; Servis, K. L. *J. Org. Chem.* **1970**, *35*, 3195.
(37) See the supplementary material for a comparison of observed and literature values of melting points.

Kinetic HH/HD/DH/DD Isotope Effects on Nondegenerate Stepwise Reversible Double Proton Transfer Reactions. NMR Study of the Tautomerism of *meso*-Tetraphenylchlorin

Martin Schlabach,[†] Gerd Scherer, and Hans-Heinrich Limbach*,[‡]

Contribution from the Institut für Physikalische Chemie der Universität Freiburg i. Br., Albertstrasse 21, D-7800 Freiburg, F.R.G. *Received August 6, 1990*

Abstract: The tautomerism of *meso*-tetraphenylchlorin-$^{15}N_4$ (TPC) has been studied by dynamic ^1H NMR spectroscopy. Only two degenerate tautomers of TPC, AC and CA, are observed whose structure corresponds to 5,10,15,20-tetraphenyl-7,8-dihydroporphyrin. Thus, the IUPAC name 5,10,15,20-tetraphenyl-2,3-dihydroporphyrin proposed for TPC is incorrect. Both tautomers interconvert via a mutual proton exchange process along two different routes. The rate constants of the tautomerism are given by $k^{HH}_{AC\rightarrow CA} = 10^{11.4\pm0.2} \exp(-58.4 \pm 1.4 \text{ kJ mol}^{-1}/RT)$, 298 K $\leq T \leq$ 406 K, $k^{HH}_{AC\rightarrow CA}(298) \approx 15\ s^{-1}$, and $k^{HD}_{AC\rightarrow CA} = 10^{11.5\pm0.3} \exp(-61 \pm 2 \text{ kJ mol}^{-1}/RT)$, 329 K $\leq T \leq$ 411 K, $k^{HD}_{AC\rightarrow CA}(298) \approx 5.8\ s^{-1}$, with an unusually small kinetic HH/HD isotope effect of $k^{HH}_{AC\rightarrow CA}/k^{HD}_{AC\rightarrow CA} \approx 2.6$ at 298 K. A theory of kinetic HH/HD/DD isotope effects for nondegenerate stepwise reversible double proton transfer reactions is described that can accommodate these kinetic results. Thus evidence is obtained that the proton transfer mechanism in TPC is stepwise as in the case of porphyrins. The analysis leads to the following conclusions. Both proton exchange routes are equivalent in the case of TPC-H_2 but nonequivalent in the case of TPC-HD. In the HD reaction a H isotope is in flight in the rate-limiting step of route i but a D isotope is in flight in the rate-limiting step of route ii. Therefore, the D route contributes only to a minor extent to the HD reaction. The observed kinetic HH/HD isotope effect arises, therefore, not from an intrinsic kinetic isotope effect but from the circumstance that in the HH case there are two equivalent H reaction routes and in the HD case there is only one H reaction route.

Introduction

Using dynamic NMR spectroscopy it has been possible in recent years to measure full kinetic HH/HD/DD isotope effects of degenerate intra- and intermolecular double proton transfer reactions of the type shown in Figure 1.[1-7] In all cases deviations from the so-called "rule of the geometric mean" (RGM) were observed. The latter states for the isotopic rate constants that[2,8-12]

$$k^{HD} = k^{DH} = (k^{HH}k^{DD})^{1/2}, \quad \text{i.e.,} \quad k^{HH}/k^{HD} = k^{HD}/k^{DD} \quad (1)$$

This rule is expected to be valid in good approximation for concerted double proton transfers, not only for the degenerate case

[†] Present address: Norwegian Institut for Air Research, PO Box 64, N-2001 Lillestrøm, Norway.
[‡] Present address: Institut für Organische Chemie, Takustr. 3, D-1000 Berlin 33, F.R.G.

(1) Limbach, H. H. Dynamic NMR Spectroscopy in the Presence of Kinetic Hydrogen/Deuterium Isotope Effect. In *NMR-Basic Principles and Progress*; Springer: Heidelberg, 1991; Vol. 23, pp 63-164.
(2) Limbach, H. H.; Hennig, J.; Gerritzen, D.; Rumpel, H. *Faraday Discuss. Chem. Soc.* **1982**, *74*, 229.
(3) Gerritzen, D.; Limbach, H. H. *J. Am. Chem. Soc.* **1984**, *106*, 869.
(4) Limbach, H. H.; Meschede, L.; Scherer, G. *Z. Naturforsch.* **1989**, *44a*, 459.

0002-7863/91/1513-3550$02.50/0

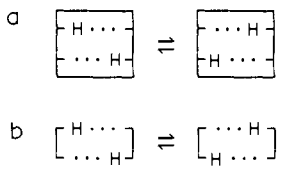

Figure 1. Intramolecular (a) and intermolecular (b) symmetric double proton transfer reactions studied by dynamic NMR spectroscopy.

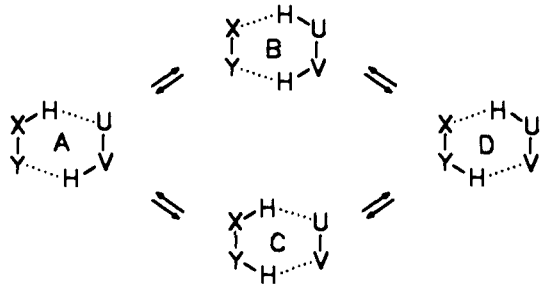

Figure 2. Stepwise double proton transfer reaction A ⇌ D involving metastable intermediates B and C.

but also for asymmetric reactions with equilibrium constants of $K \neq 1$. Although the deviations from the RGM were substantial in the case of the intermolecular reactions studied,[2-4] each of the two protons induced a primary kinetic isotope effect P to the reaction rates. This result could be explained with a mechanism where both protons are in flight during the rate-limiting reaction step and by the presence of thermally activated proton tunneling.[2-4] In the cases of the degenerate intramolecular reactions studied[2,5-7] the deviations from the RGM were larger since it was found that

$$k^{HH} \gg k^{HD} = k^{DH} \cong 2k^{DD} \qquad (2)$$

By use of formal kinetics this result could be modeled[2,5] in terms of a stepwise proton motion as shown in Figure 2 where the reactant A and the product D interconvert via two consecutive single proton transfer steps involving an intermediate, either B or C. In each elementary step the proton in flight contributes a primary kinetic isotope effect P and the bound proton a secondary kinetic isotope effect S to the reaction rates. Depending on the type of reaction studied, P was found to be enhanced by proton tunneling.[7] This interpretation of stepwise intramolecular double proton transfer was further corroborated independently by observing strong kinetic solvent effects in one case where the intermediate was expected to have a zwitterionic structure.[6]

The result of eq 2 applies, however, only to the case where the reactant A and the product D as well as the two intermediates B and C are degenerate. In this study we explore, therefore, theoretically and experimentally the more general problem of

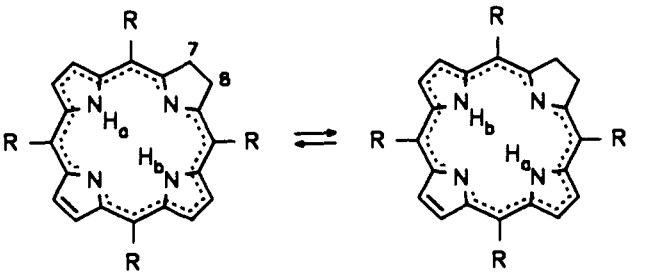

Figure 3. Mutual proton exchange in 5,10,15,20-tetraphenyl-7,8-dihydroporphyrin or 5,10,15,20-tetraphenylchlorin (TPC) where R = phenyl.

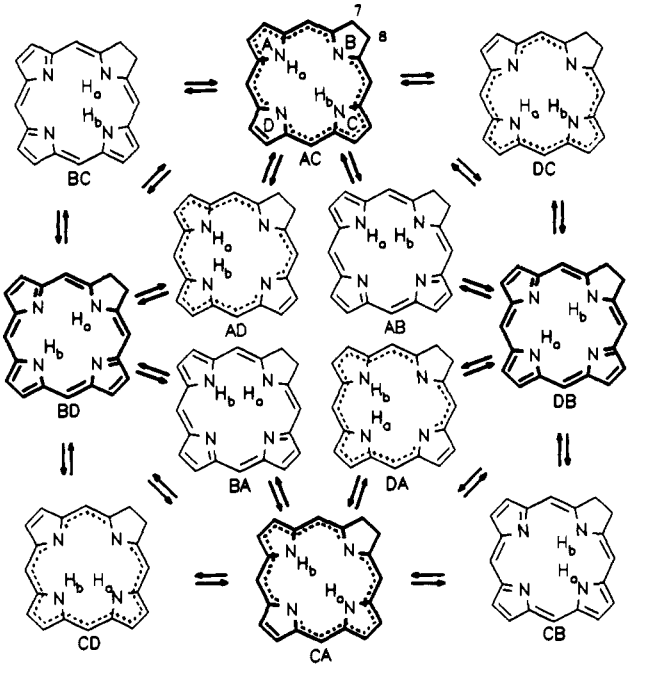

Figure 4. Extended proton transfer pathways in chlorins according to ref 17. The different tautomers are represented according to ref 18 by two capital letters MX, with M, X = A–D. M represents the pyrrole ring on which the inner proton H_a is located and X the location of H_b. All tautomers MX and XM are degenerate with exception of the case where one proton is substituted by deuterium. Only the trans tautomers AC and CA and the cis tautomers DC, DA, CD, and AD can be characterized by aromatic 18-π-electron delocalization pathways illustrated by broken lines. Spectroscopically detectable structures are boldfaced.

multiple kinetic hydrogen/deuterium isotope effects in stepwise double proton transfer reactions in the case where the equilibrium constant of the reaction studied is no longer unity. k^{HD} and k^{DH} are then no longer equivalent as in the degenerate case. Nondegenerate double proton transfer reactions play an important role in a number of organic and biochemical reactions systems.[9-12] A theory of kinetic isotope effects of such reactions has been developed by Albery et al.[10,11] in a form convenient for use in kinetic studies of irreversible reactions. We will adapt here the theory for use in dynamic NMR spectroscopy of reversible reactions. The theory will be applied to evaluate the kinetic isotope effects of the tautomerism of the inner protons in 5,10,15,20-tetraphenylchlorin (TPC) according to Figure 3. Evidence for this process was found recently by NMR line-shape analysis of the inner proton signal of ^{15}N-labeled TPC dissolved in organic solvents.[17] Note that chlorins are also subject to phototautomerism in the solid state.[18] The full proton transfer pathways of the chlorin tautomerism are shown in Figure 4. This reaction

(5) Rumpel, H.; Limbach, H. H. *J. Am. Chem. Soc.* **1989**, *111*, 5429. Rumpel, H.; Limbach, H. H.; Zachmann, G. *J. Phys. Chem.* **1989**, *93*, 1812.
(6) Scherer, G.; Limbach, H. H. *J. Am. Chem. Soc.* **1989**, *111*, 5946.
(7) Schlabach, M.; Wehrle, B.; Braun, J.; Scherer, G.; Rumpel, H.; Limbach, H. H., unpublished results.
(8) Bigeleisen, J. *J. Chem. Phys.* **1955**, *23*, 2264.
(9) Gandour, R. L.; Schowen, R. L. *Transition States of Biochemical Processes*; Plenum Press: New York, 1978.
(10) Albery, W. J. *Prog. React. Kinet.* **1967**, *4*, 355. Albery, W. J. *J. Phys. Chem.* **1986**, *90*, 3774.
(11) Belasco, J. G.; Albery, W. J.; Knowles, J. R. *Biochemistry* **1986**, *25*, 2529; **1986**, *25*, 2552.
(12) Ahlberg, P.; Jannē, K.; Löfås, S.; Nettelblad, F.; Swahn, L. *J. Phys. Org. Chem.* **1989**, *2*, 429.
(13) Crosswell, M. J.; Harding, M. M.; Sternhell, S. *J. Am. Chem. Soc.* **1986**, *108*, 3608.
(14) Crosswell, M. J.; Field, L. D.; Harding, M. M.; Sternhell, S. *J. Am. Chem. Soc.* **1987**, *109*, 2335.
(15) Schlabach, M.; Wehrle, B.; Limbach, H. H.; Bunnenberg, E.; Knierzinger, A.; Shu, A. Y. L.; Tolf, B. R.; Djerassi, C. *J. Am. Chem. Soc.* **1986**, *108*, 3856.
(16) Storm, C. B.; Teklu, Y. *J. Am. Chem. Soc.* **1972**, *94*, 1745. Storm, C. B.; Teklu, Y. *Ann. N.Y. Acad. Sci.* **1973**, *206*, 631.
(17) Schlabach, M.; Rumpel, H.; Limbach, H. H. *Angew. Chem.* **1989**, *101*, 84; *Angew. Chem., Int. Ed. Engl.* **1989**, *28*, 78.
(18) Burkhalter, F. A.; Meister, E. C.; Wild, U. *J. Phys. Chem.* **1987**, *91*, 3228.

network includes all possible intermediates of the reaction. The different tautomers in Figure 4 are characterized by the type of pyrrole unit to which they are attached. Because of the chemical perturbation, the tautomers BD (DB) and the tautomers AC (CA) are no longer equivalent, in contrast to the symmetrically substituted porphyrins. As mentioned above eq 2 was found to be valid for the latter, indicating a stepwise proton transfer mechanism.[7] It was now interesting for us to see how the kinetic isotope effects are influenced by chemical perturbation.

This paper is organized as follows. First we describe the theory of kinetic HH/HD/DH/DD isotope effects of the general stepwise double proton transfer reaction shown in Figure 2. Then we show that for the evaluation of the kinetic isotope effects the complex reaction network of chlorin shown in Figure 4 can be reduced to the simpler network of Figure 2. We then describe the experimental details of the synthesis of ^{15}N-labeled TPC and of the dynamic NMR experiments. After the Experimental Section the results on TPC are presented and discussed.

Theoretical Section

In the first part of this section we derive expressions for the kinetic HH/HD/DH/DD isotope effects of the reaction network in Figure 2, where B and C are intermediates of the reaction from A to D. We consider the case of a reversible reaction with an equilibrium constant $K_{AD} \neq 1$. In previous studies either the symmetric case[4] with $K_{AD} = 1$ or the irreversible case[10-12] with $K_{AD} \rightarrow \infty$ was treated. In the second part we consider a more complicated reaction network, which applied to the case of TPC. Note that all results are based on formal kinetics; thus, no reference is made to a particular kinetic theory such as transition state or tunneling theories, although we will use the former in order to illustrate some results. As a consequence, the equations derived are valid both for reactions over the barrier and for the case of tunneling.

Kinetic HH/HD/DH/DD Isotope Effects in the Case of a Double Proton Transfer Involving Two Stable and Two Metastable Tautomeric States. Using the usual steady-state approximation for the intermediates, one can easily derive the following expression for rate constants of the overall reaction A to D in Figure 2:

$$k_{A\rightarrow D}^{L_aL_b} = \frac{k_{A\rightarrow B}^{L_aL_b} k_{B\rightarrow D}^{L_bL_b}}{k_{B\rightarrow A}^{L_aL_b} + k_{B\rightarrow D}^{L_bL_b}} + \frac{k_{A\rightarrow C}^{L_aL_b} k_{C\rightarrow D}^{L_bL_b}}{k_{C\rightarrow A}^{L_aL_b} + k_{C\rightarrow D}^{L_bL_b}} \quad (3)$$

Note that $k_{A\rightarrow D}^{L_aL_b}$ is a double proton transfer rate constant where L_a is the isotope transferred in site a of the molecule (e.g., between X and U in Figure 2) and L_b the isotope transferred in site b (e.g., between Y and V in Figure 2). By contrast, all kinetic quantities on the right-hand side of eq 3 are single hydrogen transfer rate constants. Then, L_a is the proton in flight and L_b the bound hydrogen isotope, the nonreactive mobile proton site.

Let us define the primary and secondary kinetic isotope effects $P_{i\rightarrow j}^{L}$ and $S_{i\rightarrow j}^{L}$

$$P_{i\rightarrow j}^{L} = k_{i\rightarrow j}^{HL}/k_{i\rightarrow j}^{DL}, \qquad S_{i\rightarrow j}^{L} = k_{i\rightarrow j}^{LH}/k_{i\rightarrow j}^{LD} \quad (4)$$

Note that in the absence of isotopic fractionation between all reactants and intermediates, i.e., in the absence of equilibrium isotope effects between the latter, the following relations hold

$$P_{i\rightarrow j}^{H} = P_{j\rightarrow i}^{H} = P_{i\rightarrow j}^{D} = P_{j\rightarrow i}^{D} = P, \qquad S_{i\rightarrow j}^{H} = S_{j\rightarrow i}^{H} = S_{i\rightarrow j}^{D} = S_{j\rightarrow i}^{D} = S \quad (5)$$

It is convenient to define according to Albery[10] splitting factors of the type

$$\kappa_1 = k_{A\rightarrow B}^{HH}/k_{A\rightarrow C}^{HH}, \quad \kappa_2 = k_{D\rightarrow C}^{HH}/k_{D\rightarrow B}^{HH}, \quad \kappa_3 = \kappa = k_{B\rightarrow A}^{HH}/k_{B\rightarrow D}^{HH}, \quad \kappa_4 = k_{C\rightarrow D}^{HH}/k_{C\rightarrow A}^{HH} \quad (6)$$

By introducing eqs 4 and 6 into eq 3 one can obtain expressions for $k_{A\rightarrow D}^{L_aL_b}$, listed as eqs A7–A11 in the Appendix. In order to discuss eq A7–A11, it is useful to have a look at some special cases.

Double-Sided Degenerate Stepwise Double Proton Transfer. If A and D as well as B and C are degenerate it follows that

$$\kappa_1 = \kappa_2 = \kappa_3 = \kappa_4 = 1 \quad (7)$$

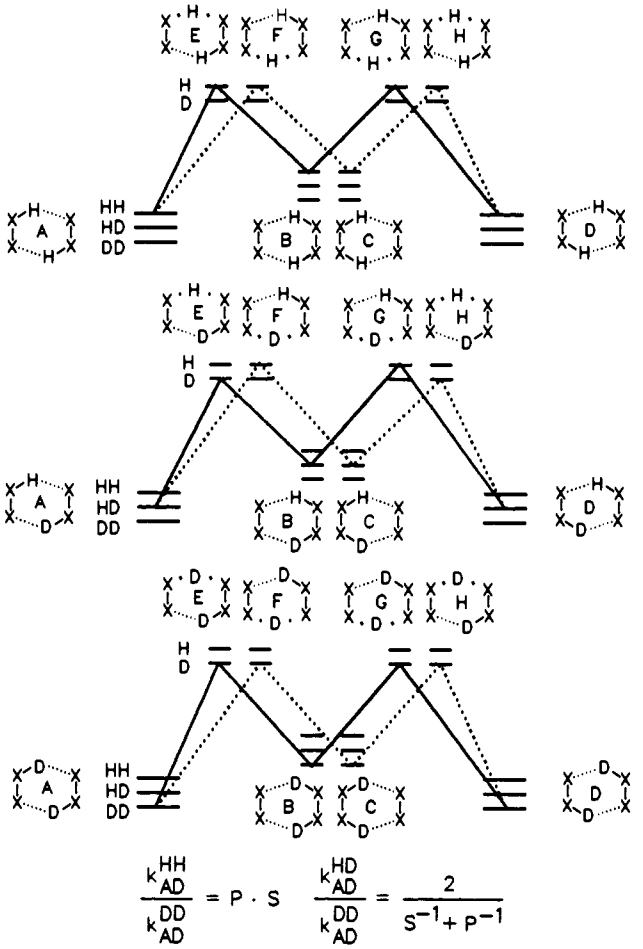

Figure 5. Free energy diagram for a degenerate stepwise double hydrogen transfer reaction according to Figure 2 and eqs 8–10. The secondary kinetic isotope effect S was set to unity.

Assuming the validity of eq 5, eqs A7–A11 simplify then to the following expressions derived previously:[5]

$$k_{A\rightarrow D}^{HH} = k_{A\rightarrow B}^{HH} \quad (8)$$

$$k_{A\rightarrow D}^{HD} = k_{A\rightarrow D}^{DH} = \frac{2}{P+S} k_{A\rightarrow B}^{HH} = \frac{2}{P^{-1}+S^{-1}} k_{A\rightarrow B}^{DD} \quad (9)$$

$$k_{A\rightarrow D}^{DD} = (PS)^{-1} k_{A\rightarrow B}^{HH} \quad (10)$$

For the case where $P \gg 1$ and $S \cong 1$, eq 2 follows directly from eqs 8–10.

Equations 8–10 can be visualized in the free energy diagram shown in Figure 5. In all isotopic processes there are two equivalent pathways via either intermediate B or C. The initial and final states A and D as well as the two intermediates B and C have two bound hydrogen isotopes, leading to three isotopic states of different energy, containing either mobile HH, HD, or DD isotopes. By contrast, the states where one hydrogen isotope is in flight are characterized by only two isotopic states of different energy because there is only one bound hydrogen isotope. Note that the term "state with a hydrogen isotope in flight" can be either a conventional transistion state or a state where the isotope tunnels from an thermally activated state through the reaction energy barrier. Let us first compare the HH and the DD reaction profiles in Figure 5. Both profiles are symmetric. Therefore, a problem of internal return arises in the sense that the intermediate reacts to D only with a probability of $^1/_2$ and returns with the same probability to A. The factor of $^1/_2$ entering the expession for $k_{A\rightarrow D}^{HH}$ and $k_{A\rightarrow D}^{HD}$ is, however, canceled in eqs 8 and 10 because there are two equivalent pathways via B and via C for all isotopic reactions. The DD reaction is slower than the HH reaction because of the loss of zero point energy of the XH/XD stretching vibration in the transition states. By contrast, the reaction profile of the HD

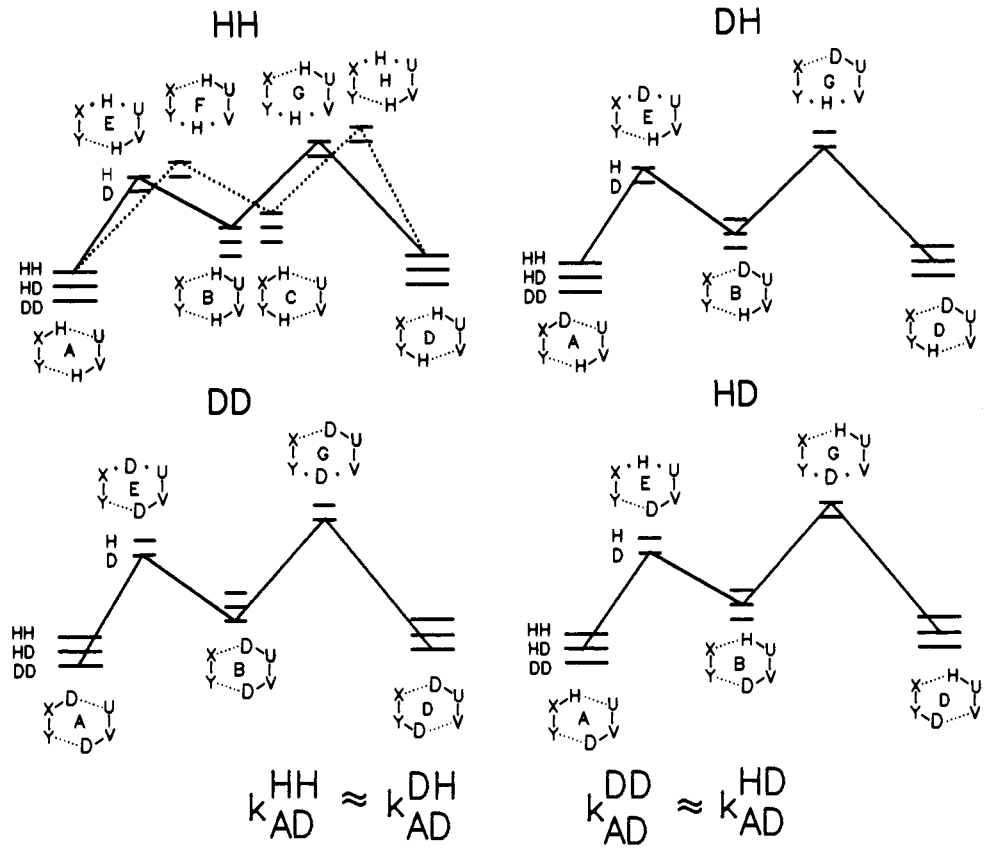

Figure 6. Free energy diagram for a nondegenerate stepwise double hydrogen transfer reaction according to Figure 2 and eqs 16–19. The secondary kinetic isotope effect S was set to unity.

process is asymmetric and the transition states E and G (and F and H) are now no more equivalent. Therefore, the problem of internal return is absent. If one neglects secondary kinetic isotope effects, the energy necessary to reach the H transition states is similar to that in the HH process and the energy necessary to reach the D transition states is similar to that in the DD case. The D transfer step constitues, therefore, the rate-limiting step of the reaction. The HD reaction has then the same free energy of activation as the DD reaction; however, since in the HD reaction all molecules that have passed the transition state react to products by contrast to the DD reaction, it follows that $k_{A\rightarrow D}^{HD} \cong 2k_{A\rightarrow D}^{DD}$ (eq 2). Note that eqs 8–10 were found to accommodate the kinetic data of the degenerate double proton transfers in azophenine,[5] porphyrins,[2,7] and oxalamidine.[6] In the latter case this interpretation of a stepwise proton motion could be further corroborated by finding strong kinetic solvent effects due to the formation of highly polar intermediates B and C.[6]

Single-Sided Asymmetric Stepwise Double Proton Transfer. Let us consider now another limiting case of eqs A7–A11, where the intermediate C as well as the transition states F and H has considerably higher free energy as compared to intermediate B and to transition states E and G. In addition, let the equilibrium constant K_{AD} be <1. Thus

$$\kappa_1 \gg \kappa_4 \qquad \kappa_3 = \kappa \not\approx 1 \tag{11}$$

From eqs A7–A11 it follows for the case where equilibrium isotope effects are absent that

$$k_{A\rightarrow D}^{HH} = \frac{1}{1+\kappa} k_{A\rightarrow B}^{HH} \tag{12}$$

$$k_{A\rightarrow D}^{HD} = \frac{1}{P\kappa + S} k_{A\rightarrow B}^{HH} \tag{13}$$

$$k_{A\rightarrow D}^{DH} = \frac{1}{S\kappa + P} k_{A\rightarrow B}^{HH} \tag{14}$$

$$k_{A\rightarrow D}^{DD} = \frac{1}{(1+\kappa)PS} k_{A\rightarrow B}^{HH} \tag{15}$$

Let us first discuss the case where A and D are degenerate, i.e., where $\kappa = 1$. The results are similar to eqs 8–10, with the difference that the right-hand sides of eqs 8–10 are multiplied by a factor of $^1/_2$. This result means that, in practice, a single- and a double-sided degenerate proton transfer cannot be distinguished experimentally.

Let us now discuss another limiting case of eqs 12–15 where $\kappa \gg 1$. Then

$$k_{A\rightarrow D}^{HH} = k_{A\rightarrow B}^{HH}/\kappa = (k_{A\rightarrow B}^{HH}/k_{B\rightarrow A}^{HH}) k_{B\rightarrow D}^{HH} = K_{AB} k_{B\rightarrow D}^{HH} \tag{16}$$

$$k_{A\rightarrow D}^{HD} = k_{A\rightarrow B}^{HH}/(P\kappa) = K_{AB} k_{B\rightarrow D}^{HH}/P \cong k_{A\rightarrow D}^{DD} \tag{17}$$

$$k_{A\rightarrow D}^{DH} = k_{A\rightarrow B}^{HH}/(S\kappa) = K_{AB} k_{B\rightarrow D}^{HH}/S \cong k_{A\rightarrow D}^{HH} \tag{18}$$

$$k_{A\rightarrow D}^{DD} = k_{A\rightarrow B}^{HH}/(PS\kappa) = K_{AB} k_{B\rightarrow D}^{HH}/(PS) = k_{A\rightarrow D}^{HH}/(PS) \tag{19}$$

These results can again be visualized in a free energy diagram as shown in Figure 6. Let us first consider the HH reaction. Since the transition state H is higher in energy than G, the pathway characterized by the broken line does not contribute to the reaction rates. For the sake of simplicity, this pathway is, therefore, no longer discussed in the other isotopic reactions; only the favored pathway characterized by the solid line that involves the transition states E and G is considered further. Since $\kappa \gg 1$, transition state E does not influence the reaction rates but only the equilibrium A $\rightleftharpoons$ B. The true transition state of the reaction in all isotopic reactions is G. The DD reaction is slower than the HH reaction because in the DD case one needs one more XH/XD zero point energy difference in order to reach G than in the HH case. Thus, neglecting secondary kinetic isotope effects, the DH reaction is as fast as the HH reaction. By contrast, in the HD reaction the D isotope is transferred in the rate-limiting step. Therefore, the HD reaction is as slow as the DD reaction.

Double Hydrogen Transfer Including Mutual Proton Exchange. In this section we expand the reaction network of Figure 2 and allow the mutual exchange of the two jumping protons according to Figure 7. This case is relevant for the tautomerism of asymmetrically substituted porphyrins[13–15] and of chlorins.[16,17] We will

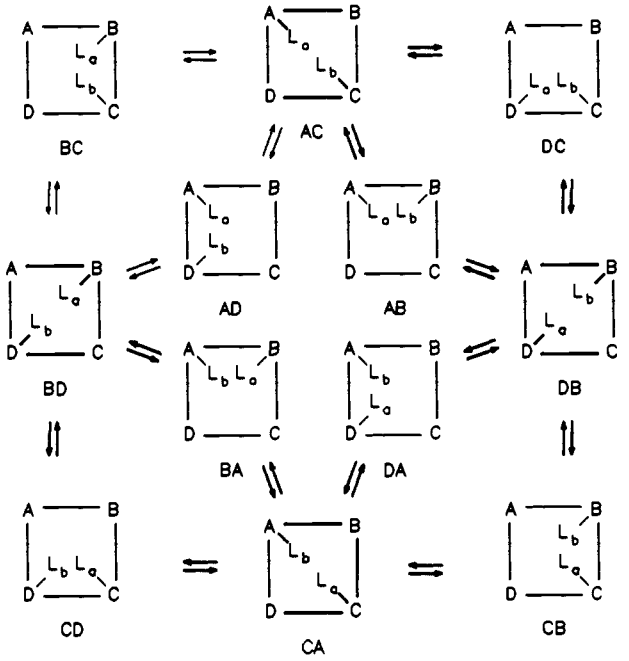

Figure 7. Extended double proton transfer reaction with four stable and eight metastable states. L_aL_b = HH, HD, DH, or DD.

show that in the presence of molecular symmetry the network of Figure 7 can be reduced to the network of Figure 2 as far as the evaluation of kinetic isotope effects is concerned.

In order to define the different processes in Figure 7 we have to expand our notation. It has been shown useful in the case of chlorins[17,18] to denote the tautomers in Figure 7 with a two letter combination MX, where M, X = A, B, C, or D. M characterizes the binding position of the hydrogen isotope L_a, X the position of L_b, where L_a, L_b = H or D. During the reaction $ML_aXL_b \rightarrow NL_aYL_b$ the hydrogen isotopes L_a and L_b jump from position M and X to N and Y. The rate of this process can then be written as

$$k_{ML_aXL_b \rightarrow NL_aYL_b} \equiv k^{L_aL_b}_{MX \rightarrow NY} \equiv k^{LL}_{MX \rightarrow NY} \tag{20}$$

Because of the different notation used here, eq 3 becomes

$$k^{LL}_{MX \rightarrow NY} = \frac{k^{LL}_{MX \rightarrow MY} k^{LL}_{MY \rightarrow NY}}{k^{LL}_{MY \rightarrow MX} + k^{LL}_{MY \rightarrow NY}} + \frac{k^{LL}_{MX \rightarrow NX} k^{LL}_{NX \rightarrow NY}}{k^{LL}_{NX \rightarrow MX} + k^{LL}_{NX \rightarrow NY}} \tag{21}$$

Note that $k^{LL}_{MX \rightarrow NY}$ describes a double proton transfer and $k^{LL}_{MX \rightarrow NX}$ and $k^{LL}_{MX \rightarrow MY}$ single proton transfers. The primary kinetic isotope effects are defined by

$$P^L_{MX \rightarrow MY} = k^{LH}_{MX \rightarrow MY}/k^{LD}_{MX \rightarrow MY}, \quad P^L_{MX \rightarrow NX} = k^{HL}_{MX \rightarrow NX}/k^{DL}_{MX \rightarrow NX} \tag{22}$$

and the secondary by

$$S^L_{MX \rightarrow MY} = k^{HL}_{MX \rightarrow MY}/k^{DL}_{MX \rightarrow MY}, \quad S^L_{MX \rightarrow NX} = k^{LH}_{MX \rightarrow NX}/k^{LD}_{MX \rightarrow NX} \tag{23}$$

In some cases the states BD and DB might not be observable, but only AC and CA are seen. Then, the observable rate would be the quadrupole proton transfer rate constant $k^{LL}_{AC \rightarrow CA}$, which depends on the double proton transfer rate constants $k^{LL}_{MX \rightarrow NY}$:

$$k^{LL}_{AC \rightarrow CA} = \frac{k^{LL}_{AC \rightarrow DB} k^{LL}_{DB \rightarrow CA}}{k^{LL}_{DB \rightarrow AC} + k^{LL}_{DB \rightarrow CA}} + \frac{k^{LL}_{AC \rightarrow BD} k^{LL}_{BD \rightarrow CA}}{k^{LL}_{BD \rightarrow AC} + k^{LL}_{BD \rightarrow CA}} \tag{24}$$

A comparison of the networks in Figures 2 and 7 shows that each of the composite double proton transfer steps in Figure 7 is equivalent to the reaction network in Figure 2 if one sets

$$A \equiv MX, \quad B \equiv NX, \quad C \equiv MY, \quad \text{and} \quad D \equiv NY \tag{25}$$

After defining splitting factors for each of the four inequivalent double proton transfer steps, one can derive a general expression for the isotopic rate constants.

We are interested here in the symmetric case that is relevant to the case of symmetrically substituted chlorins. A look at Figure 4 will convince the reader that the following relations hold for the double proton transfer rate constants in this type of reaction system:

$$k^{LL}_{DB \rightarrow AC} = k^{LL}_{DB \rightarrow CA}; \quad k^{LL}_{BD \rightarrow AC} = k^{LL}_{BD \rightarrow CA}, \quad LL = HH, HD, DH, DD \tag{26}$$

From eq 24 it follows then that

$$k^{LL}_{AC \rightarrow CA} = \tfrac{1}{2}k^{LL}_{AC \rightarrow DB} + \tfrac{1}{2}k^{LL}_{AC \rightarrow BD}, \quad LL = HH, HD, DH, DD \tag{27}$$

Furthermore, in the case of LL = HH, DD

$$k^{LL}_{AC \rightarrow CA} = k^{LL}_{AC \rightarrow DB} = k^{LL}_{AC \rightarrow BD}, \quad LL = HH, DD \tag{28}$$

Since

$$k^{HD}_{AC \rightarrow BD} = k^{DH}_{AC \rightarrow DB}, \quad k^{DH}_{AC \rightarrow CA} = k^{HD}_{AC \rightarrow CA} \tag{29}$$

it follows that

$$k^{HH}_{AC \rightarrow CA} = k^{HH}_{AC \rightarrow DB} \tag{30}$$

$$k^{HD}_{AC \rightarrow CA} = k^{DH}_{AC \rightarrow CA} = \tfrac{1}{2}k^{HD}_{AC \rightarrow DB} + \tfrac{1}{2}k^{DH}_{AC \rightarrow DB} \tag{31}$$

$$k^{DD}_{AC \rightarrow CA} = k^{DD}_{AC \rightarrow DB} \tag{32}$$

Thus, the overall quadrupole proton transfer rate constants $k^{LL}_{AC \rightarrow CA}$, LL = HH, HD, DH, DD, can be reduced to the double proton transfer rate constants $k^{LL}_{AC \rightarrow DB}$, LL = HH, HD, DH, DD, with the intermediates AB and DC. By use of the transcription A ≡ AC, B ≡ DC, C ≡ AB, and D ≡ DB, the equations of the previous paragraph can be adapted for the evaluation of the kinetic isotope effects.

The splitting factors (eq 6) are then given by

$$\kappa_1 = k^{HH}_{AC \rightarrow DC}/k^{HH}_{AC \rightarrow AB}, \quad \kappa_2 = k^{HH}_{DB \rightarrow AB}/k^{HH}_{DB \rightarrow DC}, \quad \kappa \equiv \kappa_3 = k^{HH}_{DC \rightarrow AC}/k^{HH}_{DC \rightarrow DB}, \quad \kappa_4 = k^{HH}_{AB \rightarrow DB}/k^{HH}_{AB \rightarrow AC} \tag{33}$$

For the case where the cis tautomers with a hydrogen isotope bound on site B, i.e., AB, BC, CB, and BA are considerably raised in energy as compared to the other cis tautomers, i.e., when

$$\kappa_1 = k^{HH}_{AC \rightarrow DC}/k^{HH}_{AC \rightarrow AB} \gg 1 \tag{34}$$

it follows from eq 12–15 that

$$k^{HH}_{AC \rightarrow DB} = \frac{1}{1 + \kappa} k^{HH}_{AC \rightarrow DC} \tag{35}$$

$$k^{HD}_{AC \rightarrow DB} = \frac{1}{S + P\kappa} k^{HH}_{AC \rightarrow DC} \tag{36}$$

$$k^{DH}_{AC \rightarrow DB} = \frac{1}{P + S\kappa} k^{HH}_{AC \rightarrow DC} \tag{37}$$

$$k^{DD}_{AC \rightarrow DB} = \frac{1}{1 + \kappa} \frac{1}{PS} k^{HH}_{AC \rightarrow DC} \tag{38}$$

These equations will be used to evaluate the experimental kinetic isotope effects of the tautomerism of TPC.

Experimental Section

Synthesis of ^{15}N-Labeled *meso*-Tetraphenylchlorin (TPC). For the preparation of hydroporphyrins, different methods have been proposed.[19,20] Since we wanted to study all reduction products of *meso*-tetraphenylporphyrin, i.e., *meso*-tetraphenylchlorin, *meso*-tetraphenylbacteriochlorin (TPB), and *meso*-tetraphenylisobacteriochlorin (TPiB),[17] we used the reduction of porphyrin (TPP) with diimide described by Whitlock et al.[19] with toluenesulfonic hydrazide as diimide precursor,

(19) Whitlock, H. W.; Hanover, R.; Oester, M. Y.; Bower, B. K. *J. Am. Chem. Soc.* **1969**, *91*, 7485.
(20) Harel, Y.; Manassen, J. *J. Am. Chem. Soc.* **1978**, *100*, 6228.

with a subsequent chromatographic separation of all reaction products.

The starting compound *meso*-tetraphenylporphyrin-$^{15}N_4$ (TPP) was synthesized according to Adler et al.[21] using ^{15}N-labeled pyrrole (95% ^{15}N; Fa. Hempel, Düsseldorf, Germany) as reactant. We then proceeded as follows.

In a double-necked round-bottom flask with reflux, drop funnel, and nitrogen stream, 53 mg of TPP was dissolved in 5 mL of dried and nitrogen-saturated pyridine. Then, 450 mg of dried K_2CO_3 was added. The mixture was stirred with a magnet bar and heated to 105 °C. From the funnel 500 mg of toluenesulfonic hydrazide dissolved in 25 mL of dried pyridine was added dropwise over 6 h. The reaction mixture was poured into a mixture of 100 mL of water and 200 mL of toluene and stirred on a water bath for about 1 h. The toluene phase was separated under a nitrogen stream and after cooling to room temperature it was washed with (i) 3 N ice-cold HCl, (ii) with water, (iii) with a bicarbonate solution, and (iv) twice with water. The yield was 20 mg of TPC (~40% of theory).

In order to separate the chlorin from remaining porphyrin and from bacteriochlorin, extraction with phosphoric acid[19] was found not to be practicable. The reaction products were, therefore, separated by medium-pressure liquid chromatography (MPLC) with silica (LiChroprep Si 60; Merck) as stationary phase and cyclohexane/dichloromethane as liquid phase. Since silica tends to decompose porphyrins and hydroprophyrins because of its acidity, we added 1% pyridine to the solvent in order to deactivate the solid phase.

Sample Preparation. Sealed NMR samples with a diameter of 5 mm were prepared on a vacuum line as described previously.[1,5] Both toluene-d_8, dried over potassium/sodium alloy, and tetrachloroethane-d_2 were used as solvents. The deuterium fraction in the mobile proton sites was either $D = 0$ or $D = 0.85$. The deuteration was carried out using a mixture of the CH_3OD, dried over molecular sieve, and the organic solvent.

NMR Measurements. The ^{1}H NMR spectra were measured with the pulse FT NMR spectrometers, Bruker CXP 100 working at 90.02 MHz and Bruker MSL 300 working at 300.13 MHz. The sample temperatures were calibrated before and after the NMR measurements with a PT 100 resistance thermometer (Degussa), imbedded in an NMR tube, and are estimated to be accurate to about 0.5 °C. The spectra were transferred from the Bruker Aspect 2000 and 3000 minicomputers to a PC and then to the Sperry UNIVAC 110812 computer of the Rechenzentrum der Universität Freiburg. Kinetic parameters were obtained by simulation of the spectra, as described previously[5] for the ^{1}H–^{15}N NMR signals of ^{15}N-labeled azophenine.

The initial experiments at $D = 0$ were performed with tetrachloroethane-d_2 as solvent. However, in these experiments it was found that this solvent decomposes slowly at higher temperatures. The experiments were, therefore, repeated with toluene-d_8 as solvent. No kinetic solvent effect on the reaction rates could be observed. Therefore, samples with $D = 0.85$ were prepared only with the latter solvent. Samples with $D = 0$ were measured with tetrachloroethane-d_2 and toluene-d_8 as solvents.

Results

In the first stage of this study we tried to obtain information on the tautomerism of TPC by carefully studying the NMR signals of the nonmobile protons of TPC, which should be modulated when a two-proton jump occurs in this molecule. However, these signals did not show significant changes with temperature. The β-pyrrole protons 17 and 18 (for the atom numbering see Figure 3) give rise to a singlet at $\delta = 8.34$ ppm. The hydrogen atoms 2 and 3 (as well as 12 and 13) form with the corresponding ^{15}N atoms an AA'MM'X spin system, with $\delta_{2,12} = 8.15$ ppm, $\delta_{3,13} = 8.52$ ppm, $^3J_{AM} + {}^3J_{A'M'} = 3.8$ Hz, and $^3J_{AX} = {}^3J_{MX} = 3.7$ Hz. Since these signals do not show signs of a tautomerism of the inner protons, it follows that the tautomers BD and DB in Figure 4 are not directly observable by ^{1}H NMR spectroscopy.

The line-shape analysis of the signal of the inner protons, measured at 90.02 MHz, was more successful, as shown in Figure 8. Because of the aromatic ring current this signal appears at high field, i.e., between −1 and −1.5 ppm, depending on the solvent. At room temperature the signal is split into a doublet by scalar coupling with one ^{15}N spin. Note that only one single ^{1}H–^{15}N signal is observed, which indicates that both inner hydrogen atoms of TPC have the same chemical shifts. This result is only consistent with the structures AC and CA in Figure 4. In the tautomers BD and DB as well as in all cis tautomers the inner hydrogen atoms would experience different chemical shifts. As the temperature is raised, a doublet–triplet interconversion occurs, with an exchange-broadened central triplet line. This phenomenon arises from a fast intramolecular exchange of the two inner protons. The triplet arises because in this regime, within the NMR time scale, each proton is coupled to the two ^{15}N spins of the rings A and C. No scalar coupling to the ^{15}N atoms in rings B and D is observed, indicating that the tautomers BD and DB are not populated to an observable extent, in agreement with the observations of the signals of the nonmobile protons. A small population of the latter tautomers should lead to an additional splitting of the triplet lines, as was previously found for acetylporphyrin.[15]

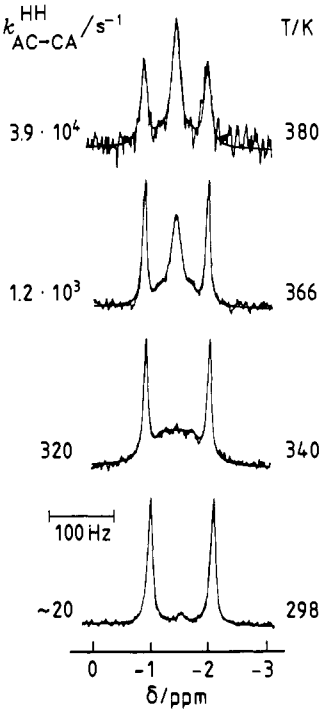

Figure 8. Superposed experimental and calculated 90-MHz ^{1}H NMR spectra of the inner protons of H_2 tetraphenylchlorin-$^{15}N_4$ as a function of temperature. The spectra stem from a ~10 mmol/L solution in tetrachloroethane-d_2 with a deuterium fraction of $D = 0$ in the inner proton sites. 3-μs $\pi/2$ pulses, 6-kHz spectral width, 3.5-s repetition rate. Reproduced with permission from ref. 17. Copyright 1989 by VCH.

Therefore, one can say that the inner proton signal of TPC is sensitive to the four-proton transfer AC → CA (see Figure 4), described by the rate constants $k^{HH}_{AC\rightarrow CA}$. By the line-shape theory described previously[1,5] these constants could be determined by simulation of the spectra at $D = 0$, as shown in Figure 8. Line-shape analysis is facilitated here by the fact that the outer lines of the triplet are not affected by the exchange; they provide, therefore, both the line width W_0 in the absence of exchange and the coupling constant $J_{^1H-^{15}N}$ needed in order to extract the kinetic information from the center line.[1,5] In the top of Figure 8 it may be noted that there is a line broadening at high temperature when tetrachloroethane-d_2 is used as solvent; this broadening is ascribed to intermolecular proton exchange due to acid impurities formed by thermal composition of the solvent; this extra line broadening is absent when using toluene-d_8 as solvent. Nevertheless, the intramolecular proton transfer rates obtained by simulation are not affected by the intermolecular exchange in the spectra of Figure 8. No kinetic solvent effect was observed within the margin of error of our experiments.

In order to obtain information on the kinetic HH/HD isotope effects on the reaction rates, a line-shape analysis of the inner proton signals of TPC was carried out at $D = 0.85$ using toluene-d_8 as solvent. Since the deuteration strongly decreased the signal to noise ratio, the experiments had to be performed at 300 MHz. The results are shown in Figure 9. Note that the use of a higher magnetic field strength does not influence the exchange-broadened

(21) Longo, F. R.; Thorne, E. J.; Adler, A. D.; Dyn, S. *J. Heterocycl. Chem.* **1975**, *12*, 1305.

Table I. Static and Dynamic Parameters of the ^1H NMR Experiments on Tetraphenylchlorin-$^{15}N_4$[a]

T/K	solvent	method	k^{HH}/s^{-1}	k^{HD}/s^{-1}	k^{DD}/s^{-1}	D	$\Delta\nu$/ppm	W_0/Hz
329.1	Tol	NH	100			0	99.5	7.0
339.2	Tol	NH	250			0	99.5	7.0
348.2	Tol	NH	400			0	99.0	9.0
354.9	Tol	NH	600			0	98.0	7.5
361.1	Tol	NH	920			0	99.5	7.3
366.6	Tol	NH	1250			0	96.0	7.0
372.0	Tol	NH	1500			0	97.5	6.5
378.6	Tol	NH	2350			0	96.0	7.0
390.4	Tol	NH	3850			0	96.0	11.0
402.8	Tol	NH	7500			0	96.0	10.0
298.1	TCE	NH	20			0	99.2	7.0
340.0	TCE	NH	320			0	99.5	7.8
366.1	TCE	NH	1180			0	99.5	7.5
383.4	TCE	NH	3600			0	99.5	8.1
393.0	TCE	NH	5000			0	99.5	12.4
406.1	TCE	NH	8000			0	99.5	17.0
329.2	Tol	NH	70[b]	55		0.85	100.0	6.5
350.9	Tol	NH	500[b]	280		0.85	99.8	11.5
374.3	Tol	NH	2000[b]	850		0.85	100.0	7.5
375.8	Tol	NH	2000[b]	900		0.85	100.0	7.2
399.1	Tol	NH	6000[b]	3000		0.85	99.5	7.9
410.9	Tol	NH	10000[b]	5000		0.85	99.5	8.4

[a] Solvent: Tol, toluene-d_8; TCE, tetrachloroethane-d_2. Method: NH, ^1H NMR line-shape analysis of the ^{15}N–^1H signals. $\Delta\nu = {}^1J_{H-^{15}N}$; $k^{LL} = k^{LL}_{AC\rightarrow CA}$, LL = HH and HD; D, deuterium fraction; W_0, determined from the nonexchanging components of the ^1H–^{15}N signal. [b] Calculated according to eq 39.

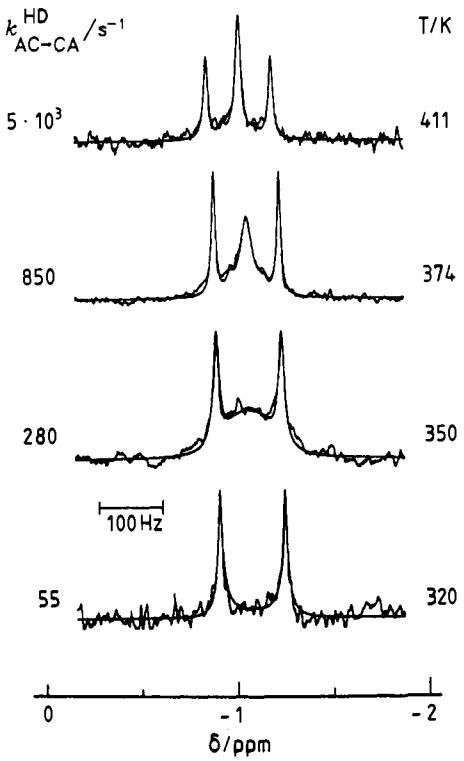

Figure 9. Superposed experimental and calculated 300-MHz ^1H NMR spectra of the inner protons of HD tetraphenylchlorin-$^{15}N_4$ as a function of temperature. The spectra stem from a ~10 mmol/L solution in toluene-d_8 with $D \approx 0.85$. Aquisition parameters as in Figure 8.

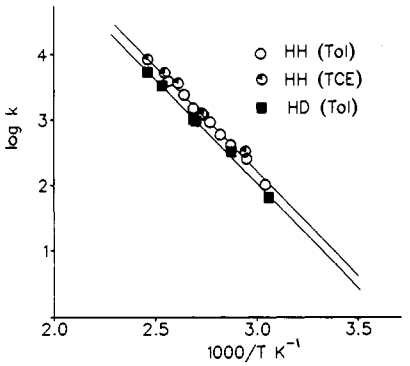

Figure 10. Arrhenius diagram of the rate constants $k = k^{LL}_{AC\rightarrow CA}$, LL = HH and HD in tetraphenylchlorin-$^{15}N_4$ dissolved in tetrachloroethane-d_2 (TCE) and toluene-d_8 (Tol).

line shape since the line broadening is due to a modulation of the scalar ^1H–^{15}N coupling and not to chemical shifts by the exchange. From the simulation of the line shapes, the rate constants $k^{HD}_{AC\rightarrow CA}$ were obtained. The known contributions of the undeuterated species were taken into account in the simulations. Note that the outer signal components are sharp at all temperatures, indicating that possible intermolecular proton exchange processes are slow within the NMR time scale.

Unfortunately, it was not possible to obtain information on the rate constants $k^{DD}_{AC\rightarrow CA}$ by ^2H NMR spectroscopy because of line broadening due to fast transverse ^2H relaxation and the small value of $J_{^2H-^{15}N}$. Since the chemical shifts of the remote ^1H, ^{13}C, and ^{15}N spins are not modulated by the exchange AC → CA and since there were no signs of the formation of the tautomers BD and DB, no attempts were made to obtain further kinetic information by ^{13}C and ^{15}N NMR spectroscopy during this study.

All kinetic results are listed in Table I from which the Arrhenius curves of the HH and the HD migration in TPC were constructed, as shown in Figure 10. A nonlinear least-squares fit of the data leads to the expressions

$$k^{HH}_{AC\rightarrow CA} = 10^{11.4\pm0.2}\exp(-58.4\pm 1.4\ \text{kJ mol}^{-1}/RT),\quad 298\ \text{K} \le T \le 406\ \text{K},\quad k^{HH}_{AC\rightarrow CA}(298) \approx 15\ \text{s}^{-1} \quad (39)$$

$$k^{HD}_{AC\rightarrow CA} = 10^{11.5\pm0.2}\exp(-61 \pm 2\ \text{kJ mol}^{-1}/RT),\quad 329\ \text{K} \le T \le 411\ \text{K},\quad k^{HD}_{AC\rightarrow CA}(298) \approx 5.8\ \text{s}^{-1} \quad (40)$$

The error margins given in eqs 39 and 40 are purely statistical and do not include any systematic errors. We calculate the following kinetic isotope effect $k^{HH}_{AC\rightarrow CA}/k^{HD}_{AC\rightarrow CA} \approx 2.6$ at 298 K.

Discussion

In the theoretical section we have described a formal theory of kinetic hydrogen/deuterium isotope effects for nondegenerate double proton transfer networks that involve composite single proton transfer steps according to Figures 2 and 7. In this discussion we will apply this theory to the tautomerism of 5,10,15,20-tetraphenylchlorin-$^{15}N_4$ (TPC, Figures 3 and 4), which was studied in the previous section by dynamic ^1H NMR spec-

troscopy. Let us first summarize the main experimental results of this study.

TPC forms in liquid solution only the degenerate tautomers AC and CA in Figure 4. Therefore, the name 5,10,15,20-tetraphenyl[$^{15}N_4$]-2,3-dihydroporphyrin proposed for TPC in the IUPAC recommendations[22] is not consistent with these findings. The correct name of TPC should read 5,10,15,20-tetraphenyl-[$^{15}N_4$]-7,8-dihydroporphyrin. At room temperature the tautomers AC and CA were found to interconvert slowly and at 380 K rapidly on the NMR time scale. The tautomers BD and DB are intermediates of this rearrangement and were not directly observable. The rate constants $k^{HH}_{AC\rightarrow CA}$ and $k^{HD}_{AC\rightarrow CA} = k^{DH}_{AC\rightarrow CA}$ were measured as a function of temperature. Besides the preliminary communication[17] neither rate constants for the proton nor for the deuteron migration in chlorins have been measured before. The kinetic HH/HD isotope effect of 2.6 at 298 K is unexpectedly small when compared to values obtained previously for other intramolecular degenerate double proton transfer reactions.[1,4-6] In the following we will explain this finding in terms of a stepwise proton transfer mechanism.

Let us first recall the kinetic data obtained for the tautomerism of *meso*-tetraphenylporphyrin (TPP),[1,2] which has been recently reinvestigated.[7] Thus, it was found that $k^{HH}_{AC\rightarrow DB}(298) \approx 2725\ s^{-1}$, $k^{HD}_{AC\rightarrow DB}(298) \approx 290\ s^{-1}$, and $k^{DD}_{AC\rightarrow DB}(298) \approx 163\ s^{-1}$, i.e.

$$k^{HH}_{AC\rightarrow DB}(298)/k^{HD}_{AC\rightarrow DB}(298) \approx 9.4,$$
$$k^{HD}_{AC\rightarrow DB}(298)/k^{DD}_{AC\rightarrow DB}(298) \approx 1.8 \quad (41)$$

These results were interpreted[7] in terms of eq 8-10, valid for a degenerate stepwise proton transfer according to Figure 2. These equations read as follows in the case of TPP:

$$k^{HH}_{AC\rightarrow DB}/k^{DD}_{AC\rightarrow DB} = PS, \quad k^{HD}_{AC\rightarrow DB}/k^{DD}_{AC\rightarrow DB} = 2/(P^{-1} + S^{-1}) \quad (42)$$

P is the primary and S the secondary kinetic isotope effect associated with the formation of the intermediates from the initial states. The temperature dependence of these quantities is given in approximation by[2,6,7]

$$P \approx 0.2 \exp(11\ \text{kJ mol}^{-1}/RT), \quad S \approx 1 \quad (43)$$

Let us now compare the rate constants of the TPP tautomerism with those of the TPC tautomerism studied here. In the theoretical section it was shown that for the rate constants of the TPC tautomerism eqs 27 and 28 hold, i.e.

$$k^{HH}_{AC\rightarrow CA} = \tfrac{1}{2}k^{HH}_{AC\rightarrow DB} + \tfrac{1}{2}k^{HH}_{AC\rightarrow BD} = k^{HH}_{AC\rightarrow DB} = k^{HH}_{AC\rightarrow BD} \quad (44)$$

where no assumption was made on whether the double proton transfers occur concerted or stepwise. Equation 44 shows that the rate constants of the HH migrations in TPP (eq 41) and TPC (eq 39) can directly be compared. Thus, we find that the double proton transfer process AC → BD is much slower in TPC as compared to in TPP. This finding can be explained as follows. By contrast to symmetric porphyrins TPC raises in energy when it reacts from AC or CA to BD or DB, because of the loss of the aromatic resonance energy. As a consequence, also the energy of the transition states for the tautomerism is raised. Extending this argument, it is straightforward that the nonaromatic cis tautomers AB and CB must have a higher energy than the aromatic cis tautomers DC and DA. Therefore, the stepwise reaction will preferentially take place via the routes (i) AC → DC → DB → DA → CA and (ii) AC → AD → BD → CD → CA. This circumstance is illustrated schematically in Figure 11 using

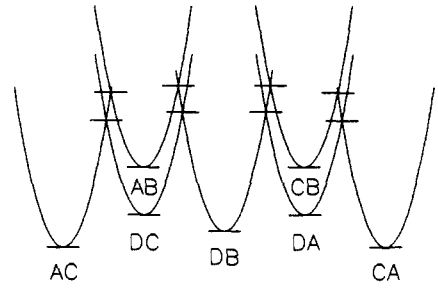

Figure 11. Schematic parabolic potential curves of the stepwise interconversion ot the chlorin tautomers AC ⇌ CA via the metastable trans intermediates DB and BD and the corresponding cis intermediates AB, DC and DA, CB.

parabolic potential curves. The rate-limiting steps of route i are the steps DC → DB and DB → DA, which involve the jump of the hydrogen isotope L_b in Figure 4. By contrast, in the rate-limiting steps AD → BD and BD → CD of route ii the isotope L_a is transferred.

In other words, eq 34 is fulfilled, which states that $\kappa_1 = k^{HH}_{AC\rightarrow DC}/k^{HH}_{AC\rightarrow AB} \gg 1$. Therefore, eqs 35-38 hold and can be introduced into eqs 30-32:

$$k^{HH}_{AC\rightarrow CA} = k^{HH}_{AC\rightarrow DB} = k^{HH}_{AC\rightarrow DC} \quad (45)$$

$$k^{HD}_{AC\rightarrow CA} = k^{DH}_{AC\rightarrow CA} = 0.5(k^{HD}_{AC\rightarrow DB} + k^{HD}_{AC\rightarrow BD}) = 0.5(k^{HD}_{AC\rightarrow DB} + k^{DH}_{AC\rightarrow DB}) = 0.5\left[\frac{1+\kappa}{S+P\kappa} + \frac{1+\kappa}{P+S\kappa}\right]k^{HH}_{AC\rightarrow CA}, \qquad \kappa \equiv \kappa_3 = \frac{k^{HH}_{DC\rightarrow AC}}{k^{HH}_{DC\rightarrow DB}} \neq 1 \quad (46)$$

P and S have the same meaning as in eq 42. $k^{HD}_{AC\rightarrow DB}$ is the rate constant along route i where the H isotope is transferred in the rate-limiting step. By constant, $k^{HD}_{AC\rightarrow BD} = k^{DH}_{AC\rightarrow DB}$ is the rate constant along route ii where the D isotope is transferred in the rate-limiting step. Therefore

$$k^{HD}_{AC\rightarrow DB} \gg k^{HD}_{AC\rightarrow BD} \quad (47)$$

Since $P \gg S \approx 1$ this means that $\kappa < 1$ in eq 46. As a consequence, route i for the case $L_a \equiv H$ and $L_b \equiv D$ is almost as fast as in the HH case where $L_a \equiv H$, $L_b \equiv H$. Thus it follows that $k^{HD}_{AC\rightarrow DB} \cong k^{HH}_{AC\rightarrow DB}$, and with eqs 46 and 47 it follows that

$$k^{HD}_{AC\rightarrow CA} \cong \tfrac{1}{2}k^{HH}_{AC\rightarrow CA} \quad (48)$$

Equation 48 is already very close to the experimental finding of $k^{HH}_{AC\rightarrow DB}/k^{HD}_{AC\rightarrow DB} = 2.6$; thus, assuming a stepwise proton transfer mechanism, the unexpected kinetic HH/HD isotope effect of the TPC migration can easily be explained. A nonlinear least-square fit of the Arrhenius curves of the TPC migration to eqs 46 and 47 using eq 43 leads to a rough estimate of the splitting factor

$$\kappa \approx 0.005 \exp(20.8\ \text{kJ mol}^{-1}/RT), \quad \kappa(298) \approx 22.1 \quad (49)$$

This means that the second step of the reactions AC → DB and CA → DB in TPC is slower than the first as expected from Figure 11. The calculated Arrhenius curves are almost indistinguishable from the solid curves in Figure 10, obtained by linear least-squares fitting.

In other words, the unexpectedly small kinetic HH/HD isotope effect of the TPC tautomerism AC → CA is not the result of a small intrinsic kinetic hydrogen/deuterium isotope effect but of the following circumstance. In the HH reaction there are two independent equivalent routes, AC → DC → DB → DA → CA (i) and AC → AD → BD → CD → CA (ii), for the interconversion. In the HD reaction AC and CA mainly interconvert by route i, where a H isotope is transferred in both rate-limiting steps AD → BD and BD → CD. The rate along this route is as fast as in the HH reaction. However, route ii no longer contributes efficiently to the reaction because a deuteron is transferred in the rate-limiting step of the reaction. Thus, the rate of the HD reaction is approximately half of the rate of the HH reaction.

(22) Moss, G. P. *Pure Appl. Chem.* **1987**, *59*, 779.
(23) Hennig, J.; Limbach, H. H. *J. Magn. Reson.* **1982**, *49*, 322.
(24) Rawling, D. C.; Davidson, E. R.; Gouterman, M. *Theor. Chim. Acta* **1982**, *61*, 227.
(25) Limbach, H. H.; Hennig, J.; Kendrick, R. D.; Yannoni, C. S. *J. Am. Chem. Soc.* **1984**, *106*, 4059.
(26) Wehrle, B.; Limbach, H. H.; Köcher, M.; Ermer, O.; Vogel, E. *Angew. Chem.* **1987**, *99*, 914.
(27) Bell, R. P. *The Tunneleffect in Chemistry*; Chapman and Hall: London, 1980.
(28) Caldin, E.; Gold, V. *Proton Transfer*; Chapman and Hall: London, 1975.

Routes involving the nonaromatic intermediates AB, CB, BC, and BA do not contribute to the reaction rates.

Conclusions

A theory of kinetic HH/HD/DH/DD isotope effects on nondegenerate stepwise double proton transfer reactions has been adapted and applied to the tautomerism of 5,10,15,20-tetraphenylchlorin, for which rate constants including kinetic HH/HD isotope effects have been measured by dynamic NMR spectroscopy. It is expected that this theory is able to accommodate the kinetic HH/HD/DD isotope effects of tautomerism in asymmetrically substituted porphyrins and related compounds.

Acknowledgment. We thank the Deutsche Forschungsgemeinschaft, Bonn-Bad Godesberg, and the Fonds der Chemischen Industrie, Frankfurt, for financial support.

Appendix

By combining eqs 4 and 3 it follows with $(P^L)^{-1} = \bar{P}^L$ and $(S^L)^{-1} = \bar{S}^L$ that

$$k^{HH}_{A\to D} = \frac{k^{HH}_{A\to B}k^{HH}_{B\to D}}{k^{HH}_{B\to A} + k^{HH}_{B\to D}} + \frac{k^{HH}_{A\to C}k^{HH}_{C\to D}}{k^{HH}_{C\to A} + k^{HH}_{C\to D}} \tag{A1}$$

$$k^{HD}_{A\to D} = \frac{\bar{S}^H_{A\to B}k^{HH}_{A\to B}\bar{P}^H_{B\to D}k^{HH}_{B\to D}}{S^H_{B\to A}k^{HH}_{B\to A} + \bar{P}^H_{B\to D}k^{HH}_{B\to D}} + \frac{\bar{S}^H_{A\to C}k^{HH}_{A\to C}\bar{P}^H_{C\to D}k^{HH}_{C\to D}}{\bar{S}^H_{C\to A}k^{HH}_{C\to A} + \bar{P}^H_{C\to D}k^{HH}_{C\to D}} \tag{A2}$$

$$k^{DH}_{A\to D} = \frac{\bar{P}^H_{A\to B}k^{HH}_{A\to B}\bar{S}^H_{B\to D}k^{HH}_{B\to D}}{\bar{P}^H_{B\to A}k^{HH}_{B\to A} + \bar{S}^H_{B\to D}k^{HH}_{B\to D}} + \frac{\bar{P}^H_{A\to C}k^{HH}_{A\to C}\bar{S}^H_{C\to D}k^{HH}_{C\to D}}{\bar{P}^H_{C\to A}k^{HH}_{C\to A} + \bar{S}^H_{C\to D}k^{HH}_{C\to D}} \tag{A3}$$

$$k^{DD}_{A\to D} = \frac{\bar{P}^H_{A\to B}\bar{S}^D_{A\to B}k^{HH}_{A\to B}\bar{P}^H_{B\to D}\bar{S}^D_{B\to D}k^{HH}_{B\to D}}{\bar{P}^H_{B\to A}\bar{S}^H_{B\to A}k^{HH}_{B\to A} + \bar{P}^H_{B\to D}\bar{S}^D_{B\to D}k^{HH}_{B\to D}} + \frac{\bar{P}^H_{A\to C}\bar{S}^H_{A\to C}k^{HH}_{A\to C}\bar{P}^H_{C\to D}\bar{S}^D_{C\to D}k^{HH}_{C\to D}}{\bar{P}^H_{C\to A}\bar{S}^D_{C\to A}k^{HH}_{C\to A} + \bar{P}^H_{C\to D}\bar{S}^D_{C\to D}k^{HH}_{C\to D}} \tag{A4}$$

For the equilibrium constants of the reaction network in Figure 2 the following reactions hold:

$$K_{AD} = K_{AB}K_{BD} = K_{AC}K_{CD} = \frac{K^{HH}_{AB}k^{HH}_{B\to D}}{k^{HH}_{B\to A}k^{HH}_{D\to B}} = \frac{k^{HH}_{A\to C}k^{HH}_{C\to D}}{k^{HH}_{C\to A}k^{HH}_{D\to C}} \tag{A5}$$

It follows then from eq 6 that

$$\kappa_1\kappa_2 = \kappa_3\kappa_4 \quad \text{and} \quad \kappa_3 = \frac{\kappa_1\kappa_2}{\kappa_4} \tag{A6}$$

By inserting eqs 6 and A5 into eqs A1–A4 the overall rate constants $k^{L_AL_B}_{A\to D}$ can be expressed by the single rate constants $k^{HH}_{A\to B}$ or $k^{HH}_{A\to C}$

$$k^{HH}_{A\to D} = \left[\frac{\kappa_1}{1+\kappa_3} + \frac{\kappa_4}{1+\kappa_4}\right]k^{HH}_{A\to C} \tag{A7}$$

$$k^{HH}_{A\to D} = \left[\frac{1}{1+\kappa_3} + \frac{\kappa_4/\kappa_1}{1+\kappa_4}\right]k^{HH}_{A\to B} \tag{A8}$$

$$k^{HD}_{A\to D} = \left[\frac{\bar{S}^H_{A\to B}\bar{P}^H_{B\to D}}{\bar{S}^H_{B\to A}\kappa_3 + \bar{P}^H_{B\to D}} + \frac{\bar{P}^H_{A\to C}\bar{S}^H_{C\to D}\kappa_4/\kappa_1}{\bar{P}^H_{C\to A}\kappa_4 + \bar{S}^H_{C\to D}}\right]k^{HH}_{A\to B} \tag{A9}$$

$$k^{DH}_{A\to D} = \left[\frac{\bar{P}^H_{A\to B}\bar{S}^H_{B\to D}}{\bar{P}^H_{B\to A}\kappa_3 + \bar{S}^H_{B\to D}} + \frac{\bar{S}^H_{A\to C}\bar{P}^H_{C\to D}\kappa_4/\kappa_1}{\bar{S}^H_{C\to A}\kappa_4 + \bar{P}^H_{C\to D}}\right]k^{HH}_{A\to B} \tag{A10}$$

$$k^{DD}_{A\to D} = \left[\frac{\bar{P}^H_{A\to B}\bar{S}^D_{A\to B}\bar{P}^H_{B\to D}\bar{S}^D_{B\to D}\kappa_1}{\bar{P}^H_{B\to A}\bar{S}^H_{B\to A}\kappa_3 + \bar{P}^H_{B\to D}\bar{S}^D_{B\to D}} + \frac{\bar{P}^H_{A\to C}\bar{S}^D_{A\to C}\bar{P}^H_{C\to D}\bar{S}^D_{C\to D}\kappa_4/\kappa_1}{\bar{P}^H_{C\to A}\bar{S}^H_{C\to A}\kappa_4 + \bar{P}^H_{C\to D}\bar{S}^D_{C\to D}}\right]k^{HH}_{A\to B} \tag{A11}$$